PUBLICATIONS OF THE ASTRONOMICAL SOCIETY OF THE PACIFIC, **122**:1207–1213, 2010 October

PICO: Portable Instrument for Capturing Occultations

MATTHEW LOCKHART, MICHAEL J. PERSON, AND J. L. ELLIOT[1]

Department of Earth, Atmospheric, and Planetary Sciences, Massachusetts Institute of Technology, 77 Massachusetts Avenue, Cambridge, MA 02139; lockhart@mit.edu, mjperson@mit.edu, jle@mit.edu

AND

STEVEN P. SOUZA[2]

Department of Astronomy, Williams College, 33 Lab Campus Drive, Williamstown, MA 01267; ssouza@williams.edu

Received 2010 May 24; accepted 2010 July 27; published 2010 August 26

ABSTRACT. We describe a portable imaging photometer for the observation of stellar occultation events by Kuiper Belt objects (KBOs) and other small bodies. The system is referred to as the Portable Instrument for Capturing Occultations (PICO). It is designed to be transportable to remote observing sites by a single observer. A GPS timing system is used to trigger exposures of a Finger Lakes Instrumentation ML261E-25 camera to facilitate the combination of observational results from multiple sites. The system weighs a total of 11 kg when packed into its single rigid $55.1 \times 35.8 \times 22.6$ cm container, meeting current airline size and weight limits for carry-on baggage. Twelve such systems have been constructed. Nine systems were deployed for observation of a stellar occultation by Kuiper Belt object 55636 in 2009 October. During the same month, one system was used to record a stellar occultation by minor planet 762 Pulcova.

1. INTRODUCTION

1.1. Stellar Occultations

Kuiper Belt objects (KBOs) are too small and distant for their disks to be resolved by ground-based telescopes, preventing direct measurements of object radii. While it is possible to infer the radius of a given object by combining optical photometric data with infrared spectroscopic data (Stansberry et al. 2008), there is a method by which KBO radii can be measured directly. Occasionally, the combined orbital motions of a KBO and Earth will cause the object to briefly block the light from, or occult, a background star as viewed from Earth. Such events are known as stellar occultations (Elliot 1979). Repeated astrometric observation of a given object and of the strip of sky it will pass through in the near future allows prediction of such events (McDonald & Elliot 2000).

Background stars are far more distant from Earth than any Sun-orbiting occulting object. As a result, the shadow such an object casts is (as viewed from the direction of the object) effectively the same size and shape as the object itself. During an occultation this shadow sweeps across Earth's surface, resulting in a strip of Earth's surface from which the occultation is observable. An observer located within this shadow path will record a brief dimming or disappearance of the light from the background star, corresponding to a chord across the occulting object. Multiple observers distributed across the shadow path in the cross-track direction will observe multiple unique chords.

If the occulting body has an atmosphere, it may be detectable. A sufficiently detailed occultation light curve may not only reveal the presence of an atmosphere but also allow its composition and structure to be inferred (Elliot et al. 2003a, 2003b).

1.2. Observer Deployment Strategy

Occultation events are best observed from multiple stations spread out in a direction perpendicular to the centerline of the predicted shadow path (the "cross-track" direction). There are two main reasons for this. First, spreading observers out in the cross-track direction increases the likelihood of the event being observed by at least one station. The overall cross-track span of the array of stations is determined mainly by the estimated cross-track uncertainty in the event prediction. Second, while a single observed chord establishes a lower limit on the radius of an occulting object, multiple chords allow the construction of a coarse profile of the object, which in turn allows measurements of radius and oblateness to be made. A distance between stations in the cross-track direction that is less than the estimated radius of the object helps ensure that more than one station will be inside the actual shadow path. Note that the position of stations in the along-track direction is much more flexible than it is in the cross-track direction. The positions of the

[1] Also: Department of Physics, Massachusetts Institute of Technology, 77 Massachusetts Avenue, Cambridge, MA 02139.

[2] Also: Hopkins Observatory, Williams College, 33 Lab Campus Drive, Williamstown, MA 01267.

stations need not form an actual line or have any particular along-track spacing or span.

A one-sigma uncertainty of 20 mas in the position of a KBO at a distance of 40 AU translates to an uncertainty of roughly 600 km in the cross-track position of the predicted shadow path. A hypothetical campaign to observe an occultation by a KBO with a radius of 300 km might involve seven stations with a cross-track spacing of 300 km for a total cross-track span of 1800 km (two object radii plus one sigma of uncertainty on either side of the predicted centerline). Given the likelihood of some of those stations being unable to observe due to weather, the campaign would benefit from still more stations. The number of stations may also be increased in order to allow for more than one sigma of uncertainty in the position of the centerline. The successful observing campaign described by Elliot et al. (2010) incorporated 18 stations spread across 5920 km in the cross-track direction, with 11 stations having favorable weather and two of those stations observing the occultation.

Based on a sample of 29 bright KBOs and an assumption of 1 s exposures and a minimum acceptable signal-to-noise ratio (S/N) of 10, Elliot & Kern (2003) estimate that roughly six events per year should be observable by portable telescopes with apertures of 0.36 m. The number of observable events is increased by the existence of larger (though fixed) telescopes-of-opportunity in numerous locations around the world. As a result, the rate at which a given research group can observe occultations is less likely to be limited by a lack of events to observe than by the availability of funding, observers, and equipment for observation campaigns.

2. SYSTEM MOTIVATION

In order to usefully constrain the radius or shape of an occulting body, photometric data must have certain qualities. First, the occulted star should be well exposed in each (out-of-occultation) frame, providing a high per-frame S/N. Second, the exposure time of each frame should be short, and dead time between frames should be minimized, in order to record the event in detail. Third, detector read noise should be low enough that it is less significant than photon noise from the star and occulting body. Fourth, the midtimes of all exposures must be recorded accurately. If multiple stations observe an event, they must use a common time base.

Several constraints make this sort of data difficult to record. First, most occultations involve dim stars, as the sky is more densely populated with these than with bright stars. Light is in short supply and so detector quantum efficiency must be high. Second, occultations are brief, usually being visible for only a few seconds from a given site. This requires that frames be recorded at a fast cadence, further reducing the amount of light collected in each frame. Third, computers are generally poor sources of timing information. Most operating systems cannot guarantee that exposures of a detector under their control will be started or ended at precise times or precise intervals. Timing information must be obtained from a GPS timing system or some other external source.

Any given occultation event is likely to only be observable from a small fraction of Earth's dry land. As a result, observing occultations necessarily involves travel. If observers can carry their detector hardware with them as carry-on luggage, there are fewer opportunities for loss, delay, or theft of that hardware to prevent successful observations. An ideal occultation camera system must be rugged enough to endure rough handling and small and light enough to be treated as carry-on luggage. At the time of this writing the de facto standard size and weight limits for carry-on luggage in the USA are $22 \times 14 \times 9$ inches (approximately $56 \times 36 \times 23$ cm) and 40 pounds (approximately 18 kg).

The Portable Occultation, Eclipse, and Transit System (POETS) is a high-speed imaging photometer system developed jointly by Williams College and the Massachusetts Institute of Technology (MIT) (Souza et al. 2006; Gulbis et al. 2008). POETS consists of a low-read-noise Andor iXon frame-transfer camera, a GPS timing system, and a small desktop computer. Reads of the frame-transfer CCD are triggered by a configurable clock signal from the GPS. The camera provides 512×512 16 μm pixels. Frame-transfer capability virtually eliminates delay between exposures, while GPS triggering ensures that exposure midtimes are accurately known and that exposures are of equal length. The camera communicates with the computer via a custom PCI card and so a desktop computer is required.

A complete POETS system fits inside two carry-on-sized carrying cases (each having approximate dimensions $54 \times 34 \times 27$ cm) weighing a total of 30 kg and is designed to be carried by a pair of observers traveling together. POETS has been used to observe stellar occultations by Pluto and Charon (Gulbis et al. 2006; Elliot et al. 2007; Person et al. 2008).

In mid-2009 the MIT Planetary Astronomy Laboratory recognized a need for an occultation camera system which was less expensive than POETS and so could be acquired in larger numbers. The resulting system design is called the Portable Instrument for Capturing Occultations (PICO). PICO resembles POETS, but trades frame-transfer capability for drastically reduced cost ($5000 per PICO system versus $38,000 per POETS system in 2009 dollars), a roughly 50% reduction in size and weight, and an increase in ruggedness.

3. SYSTEM DESCRIPTION

Each PICO system consists of a CCD camera, a GPS timing system, and a laptop computer. Camera exposures are triggered by clock pulses generated by the GPS. The Lenovo IdeaPad S12 laptop is used to configure the camera, store frames, and control the GPS trigger signal. A system schematic is shown in Figure 1.

Portable instruments are often assembled in the dark and by observers who are new to the hardware. Fortunately, the combination of connectors used by the five signal cables and three

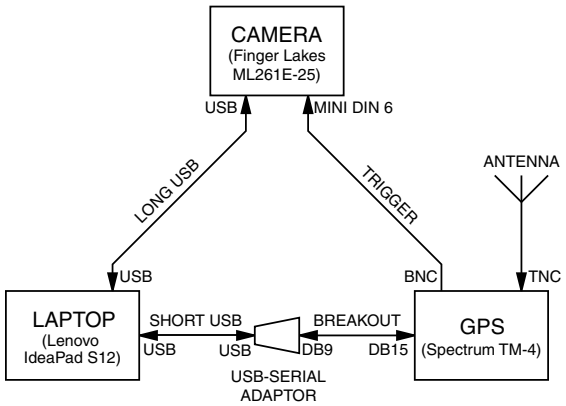

FIG. 1.—Schematic of a PICO system. The "breakout" cable connected to the GPS timing system splits the DB15 multifunction connector on the rear panel of the GPS into a DB9 serial connector and a barrel connector (not shown) for DC power input. Note that the trigger signal is independent of the computer. Note also that, except for the presence of an unused second BNC connector on the rear panel of the GPS (which will do no harm if it is inadvertently connected to the trigger cable), there is only one way to assemble the system.

power supplies renders it impossible for an observer to assemble a PICO system incorrectly in such a way that harm is done. Except for the presence of an unused second BNC connector on the rear panel of the GPS (which will do no harm if it is inadvertently connected to the trigger cable), there is only one way to assemble the system.

The switching power supplies for the laptop, camera, and GPS accept input at 100–240 V AC and 50 or 60 Hz and so can be operated nearly anywhere in the world without the need for outboard transformers. Each system is stored and carried in a foam-padded, waterproof Hardigg/Storm model iM2500 case. A complete system in its case, shown in Figure 2, has dimensions $55.1 \times 35.8 \times 22.6$ cm and weighs a total of 11 kg.

3.1. Camera

PICO uses a Finger Lakes Instrumentation ML261E-25 camera, which is based on the Kodak KAF-0261E CCD sensor. It provides 512×512 20 μm pixels. When used with a 0.36 m diameter $f/11$ Celestron SCT (a typical telescope-of-opportunity), this results in a pixel scale of $1''$ pixel^{-1}.

A three-stage thermoelectric cooling device is able to maintain the sensor at 50°C (or better) below ambient temperature, ensuring that dark current is negligibly small in the roughly 1 s exposures used in occultation observations (see § 4.1).

The sensor can be read out at either 1.0 MHz or 2.8 MHz. In either mode the read noise varies between 12 e$^-$ pixel^{-1} and 15 e$^-$ pixel^{-1} from unit to unit. In principle, reading a 512×512 array of pixels at 2.8 MHz should require just under 0.1 s. In reality, the interframe time is larger; see § 4.1 for details. Binning and subframing are supported and can be employed to reduce the amount of time lost.

FIG. 2.—A complete PICO system in its case. Cables and power supplies (not visible) are stored beneath the laptop computer at left. The camera is stored at upper right. The GPS timing system is stored at lower right. The empty recess at far lower right provides storage space for camera mounting hardware and other accessories. Wheels (at left) and a retractable towing handle (at right, not visible) reduce observer fatigue during travel.

The camera is outfitted with a Uniblitz 25 mm high-speed shutter in place of the default 41 mm shutter. This reduces the delay between the receipt of a trigger signal and the beginning of an exposure. This also reduces the vignetting effect of the shutter, which is most significant at short exposure times.

The camera is controlled by Diffraction Limited MaxIM DL software via a USB 2.0 port on the control computer. External triggering of an exposure is accomplished by momentarily raising pin 5 of the camera's mini-DIN AUX port from TTL low (0 V) to TTL high (+5 V). The external trigger signal controls the start time of each exposure and the cadence of the exposures. The duration of each exposure and the total number of exposures to be recorded remain under the control of MaxIM DL.

3.2. GPS

A Spectrum Instruments TM-4 GPS timing system is used to provide the trigger signal used by the camera. The GPS is operated from the control computer via a serial cable and a Keyspan USA-19HS USB-to-serial adaptor. Vendor-supplied software running on the control computer is used to monitor the status of the GPS (time, position, and number of satellites in use) and to control the device's "programmed output pulse" (POP)

trigger output. The POP signal is output via a BNC connector on the rear panel of the GPS. A custom-made 5 m cable carries the POP signal from the GPS to the camera. The GPS is rated to deliver timing pulses with submicrosecond accuracy.

3.3. Occultation Observation Procedure

Prior to an occultation observation, the observer powers the camera and GPS to allow the CCD to cool and the GPS to find its location and time. Recording of bias frames and twilight flat-field frames, as well as location of the target field, can be performed without the aid of GPS triggering. The observer then uses MaxIM DL to configure the camera to record a series of GPS-triggered frames, specifying the exposure time for each frame and the total number of frames to be recorded and instructing the camera to listen for trigger pulses. Next, the observer uses the GPS software to schedule a series of trigger pulses, specifying the exact start time of the series, the cadence of the pulses, and the duration of each pulse. A duration of 10 ms has proven sufficient to trigger the camera consistently. At the scheduled time the GPS will begin outputting trigger pulses and the camera will record frames in response. When the total number of frames to be recorded is reached, MaxIM DL stops recording. The GPS trigger pulse series is stopped manually by the observer.

4. OBSERVATIONS

At the time of this writing, PICO systems have been used in one attempted observation of a stellar occultation by a KBO. A summary of this attempt, testing data, and an observation of a stellar occultation by an asteroid are presented here.

4.1. Bench Testing

Gain and read noise were determined by recording two bias frames and two flat-field frames at a detector temperature of −30°C and applying the formulae from Massey & Jacoby (1992):

$$\text{gain} = \frac{(\bar{F}_1 + \bar{F}_2) - (\bar{B}_1 + \bar{B}_2)}{\sigma^2_{(F_1-F_2)} - \sigma^2_{(B_1-B_2)}} \tag{1}$$

$$\text{read noise} = \frac{\text{gain} \cdot \sigma_{(B_1-B_2)}}{\sqrt{2}}, \tag{2}$$

where $\bar{B}$ is the mean value of all pixels of a given bias frame, $\bar{F}$ is the mean value of all pixels of a given flat-field frame, $\sigma_{(F_1-F_2)}$ is the standard deviation of all pixels of the difference of two flat-field frames, and $\sigma_{(B_1-B_2)}$ is the standard deviation of all pixels of the difference of two bias frames. Gain and read-noise measurements for the 12 cameras are included in Table 1.

Dark current was determined by recording one bias frame and one 60 s dark frame at a given detector temperature and applying the formula:

$$\text{dark current} = \bar{D} - \bar{B}, \tag{3}$$

where $\bar{D}$ is the mean value of all pixels of a given dark frame and $\bar{B}$ is the mean value of all pixels of a given bias frame. Dark-current measurements for the 12 cameras are included in Table (2).

Note that, with the exception of the camera with serial number 032, the performance of the cameras is approximately within

TABLE 1
PICO Gain and Read Noise at −30°C.

		1.0 MHz		2.8 MHz	
PICO system letter	Camera serial number	Gain (e^-ADU^{-1})	Read Noise (e^-)	Gain (e^-ADU^{-1})	Read Noise (e^-)
A	017	1.95	12.9	1.81	11.7
B	012	2.31	14.9	2.10	14.8
C	032	1.98	13.6	1.83	13.9
D	059	2.37	14.5	2.18	14.6
E	036	1.92	12.9	1.86	13.5
F	044	1.97	13.2	1.80	13.4
G	008	2.00	13.2	1.82	13.4
H	004	1.99	14.0	1.84	13.9
I	011	1.99	13.4	1.80	13.2
J	040	2.02	13.6	1.85	13.5
K	013	2.00	13.4	1.82	13.4
L	058	2.25	13.3	2.05	14.0
Mean		2.06	13.6	1.90	13.6
Mfg. spec.		...	12	...	12

TABLE 2
PICO Dark Current at Various Temperatures

PICO system letter	Camera serial number	−30°C	−20°C	−10°C	0°C
		ADU minute^{-1} pixel^{-1}			
A	017	4	15	45	92
B	012	7	12	29	48
C	032	18	31	72	133
D	059	2	11	24	46
E	036	<0.5	11	29	56
F	044	1	10	26	53
G	008	6	17	36	65
H	004	3	1	24	44
I	011	6	4	19	40
J	040	<0.5	17	23	52
K	013	<0.5	5	20	40
L	058	<0.5	11	24	40
Mean		3.92	12.1	30.9	59.1
Mfg. spec. [a]		3–30	…	…	…

Note.—1.0 MHz read mode used.

[a] The manufacturer's specification of 0.1–1 e$^-$ s^{-1}pixel^{-1} at −30°C has been converted to ADU/minute/pixel using an assumed gain of 2 e$^-$ADU^{-1}.

the manufacturer's read-noise specification of 12 e$^-$ADU^{-1} and dark-current specification of 0.1–1 e$^-$s^{-1}pixel^{-1} at −30°C.

Long sequences of exposures were recorded and timed to determine the amount of interframe time required to read the CCD and store the data. These sequences were recorded in 2.8 MHz read mode and used internal triggering (in which the camera does not wait for a GPS trigger pulse before proceeding from one exposure to the next). A sequence of 120 1 s light frames, without any pixel binning, was recorded in 211 s, for an interframe time of 0.76 s frame^{-1}. A sequence of 120 0.5 s light frames, using 2 × 2 binning, was recorded in 138 s, for an interframe time of 0.65 s frame^{-1}. See Table 3 for details.

4.2. Comparison of POETS and PICO Baseline Photometry

Test light curves were obtained for a $m_v = 11$ star using both POETS and PICO. Both sets of 1 s exposures were obtained on the same night, using the same 0.36 m telescope, and at comparable air masses. No filter was used. Photometric reduction of both data sets was performed using the same comparison star and a variety of aperture radii. For both data sets an aperture radius of six pixels resulted in the lowest noise. The resulting photometric sequences are shown in Figure 3.

The per-point S/N of the PICO and POETS sequences are 73 and 79, respectively. These are similar in spite of the difference in quantum efficiency between the two detectors (the quantum efficiency of the POETS detector peaks at above 90%, while the PICO detector is rated at 58%). This is because in both sequences, given the air mass of the target field, the short exposure time, and the small telescope aperture, atmospheric scintillation noise is nearing the point at which it becomes more significant than object photon noise.

Note that, while both data sets are made up of 1 s exposures, the cadences are different. POETS, with its negligible interframe time, requires 1 s to record a 1 s exposure. PICO, with its more significant interframe time, requires 1.76 s (from Table 3). This does not affect the validity of the comparison of the two light curves in Figure 3. Were this an occultation observation, however, this would affect the S/N per unit distance for a chord across an occulting body by a factor of $\sqrt{0.76}/1.76$, or 0.50.

4.3. Occultation by Kuiper Belt Object 55636

Nine PICO systems were deployed to locations in the USA, Mexico, and Australia in preparation for a predicted stellar occultation by Kuiper Belt object 55636 on the evening of 2009 October 9 UT. This was the first deployment of the newly constructed systems. Due either to unfavorable weather or to being located outside the shadow path of the event, none of the PICO sites witnessed an occultation. Observations were carried out from all PICO sites where weather permitted, however, and no observers were prevented from observing by equipment difficulties. An occultation was witnessed by observers in Hawaii (who were equipped with other instruments) and is reported by Elliot et al. (2010).

4.4. Occultation by 762 Pulcova

In early 2009 October observer Bruce Berger was deployed with a PICO system to Observatorio Astronómico Nacional,

TABLE 3
PICO CCD read and data storage interframe time

Binning (pixels)	Frame type	Exposure time (s)	Total frames	Elapsed time (s)	Cycle time (s frame^{-1})	Interframe[a] time (s frame^{-1})
1×1	bias	…	100	71	0.71	0.71
1×1	light	1	120	211	1.76	0.76
2×2	bias	…	100	55	0.55	0.55
2×2	light	0.5	120	138	1.15	0.65

Note.—2.8 MHz read mode used. Internal triggering (in which the camera does not wait for a GPS trigger pulse before proceeding from one exposure to the next) used.

[a] Here, we define interframe time as cycle time minus exposure time.

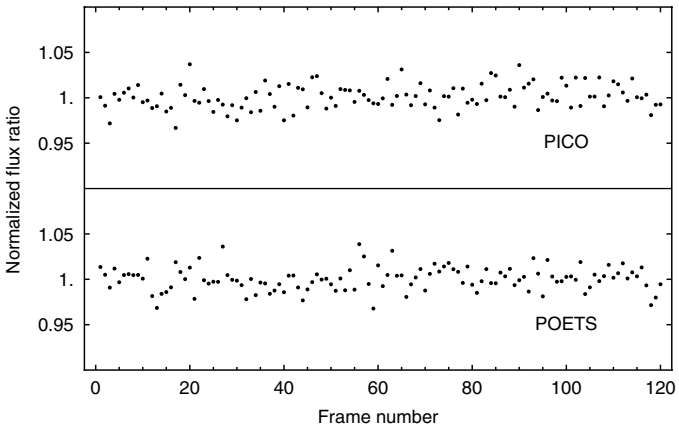

FIG. 3.—Top: Sequence of 120 1 s PICO exposures with no pixel binning. Per-point S/N = 73 for the points shown. Bottom: Sequence of 120 1 s POETS exposures with no pixel binning. Per-point S/N = 79 for the points shown. Each sequence has been normalized about its mean. Both sequences were recorded on the same evening, at comparable air masses, and using the same $m_v = 11$ target star and 0.36 m telescope. Note that, due to CCD read time and data storage overhead, each exposure cycle in the PICO sequence required 1.76 s rather than the 1 s required for each exposure cycle in the POETS sequence.

San Pedro Mártir, Baja, California, as part of the KBO occultation observing campaign described in § 4.3. Two nights before the event, on the morning of 2009 October 8 UT, he observed the occultation of a $m_r = 11.9$ star by minor planet 762 Pulcova using PICO and the 1.5 m telescope at San Pedro Mártir. Seeing was roughly 1" (FWHM). The moon was 27 deg away from the observed field and was 81% illuminated. Internal (non-GPS) triggering was used. A sequence of 1102 1 s exposures with 2×2 binning was recorded in 1794 s, for a cadence of approximately one frame per 1.63 s.

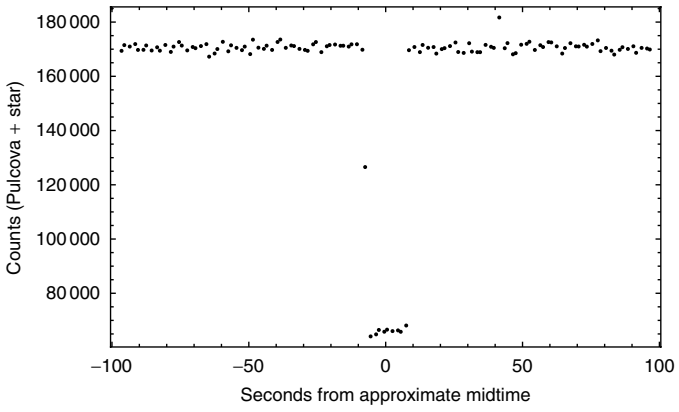

FIG. 4.—Occultation of a $m_r = 11.9$ star by minor planet 762 Pulcova on 08 2009 October UT. One-second PICO exposures with 2×2 binning and a cadence of approximately one frame per 1.63 s, 1.5 m telescope used. Each value represents the combined light from 762 Pulcova and the star. Values are unbinned in time. The outlying point occurring approximately 42 s after the midtime is the result of a particle striking the CCD inside of the photometric aperture used in reduction. S/N = 129 per point for the points shown (omitting the points recorded during the occultation itself and the one outlying point).

Our reduction of this data set, using sky-subtracted aperture photometry with an aperture radius of 40 pixels, produces the light curve shown in Figure 4. The outlying point occurring approximately 42 s after the event midtime is the result of a particle striking the CCD inside of the photometric aperture used in reduction. S/N = 129 per point for the points shown (omitting the points recorded during the occultation itself and the one outlying point).

5. CONCLUSIONS

The observed occultation event discussed in § 4.4 can be used to predict the performance of PICO when used (with comparable telescope hardware and observing conditions) to observe other events. Such scaling arguments suggest that PICO has the sensitivity required to measure the radii of KBOs and to detect the presence of atmospheres around those objects.

Given the S/N of 129 achieved using the $m_r = 11.9$ occultation star in § 4.4, the event would still have been marginally detectable (S/N = 1) using a star of $m_r = 17.2$. Given the $m_r = 11.9$ star, the observing cadence of approximately one frame per 1.63 s achieved during the event in § 4.4, a typical KBO shadow speed of 25 km s^{-1}, and the need for at least two in-occultation data points to detect an occultation, a KBO with a diameter as small as 82 km would have been detectable.

Person et al. (2008) found a density scale height (at the half-light radius) of 56.2 km for Pluto's 2007 atmosphere. They report probing a shell of atmosphere two scale heights thick. Given the observing cadence of approximately one frame per 1.63 s achieved during the event in § 4.4 and a typical KBO shadow speed of 25 km s^{-1}, 2.8 frames would have been recorded during the 2.2 s required to traverse two scale heights. This would be an insufficient number of points per scale height to usefully probe a Pluto-like KBO atmosphere, but it would be sufficient to detect the presence of such an atmosphere.

The performance of PICO does not match that of its older sibling POETS in all respects, and was never expected to. The PICO design consciously accepts a reduction in cadence (versus POETS) in exchange for lower cost (and size) in order to allow the construction of far more systems. As a result, dedicated, GPS-synchronized occultation cameras were placed at far more sites for the MIT/Williams-led 2009 October KBO occultation observation campaign than would have been possible using POETS systems alone.

Sky testing for this work was performed at the Massachusetts Institute of Technology George R. Wallace, Jr. Astrophysical Observatory in Westford, MA, and at the Williams College Hopkins Observatory in Williamstown, MA. We would like to thank Bruce Berger for his efforts in recording the 762 Pulcova occultation. This work was funded in part by NASA grant NNX07AK73G.

REFERENCES

Elliot, J. L. 1979, ARA&A, 17, 445
Elliot, J. L., & Kern, S. D. 2003, Earth Moon Planets, 92, 375
Elliot, J. L., Person, M. J., & Qu, S. 2003a, AJ, 126, 1041
Elliot, J. L., et al. 2003b, Nature, 424, 165
———. 2007, AJ, 134, 1
———. 2010, Nature, 465, 897
Gulbis, A. A. S., Elliot, J. L., Person, M. J., Babcock, B. A., Souza, S. P., & Zuluaga, C. A. 2008, in AIP Conf. Proc. 984, High Time Resolution Astrophysics: The Universe at Sub-Second Timescales ed. D. Phelan, O. Ryan, & A. Shearer (New York: AIP), 91, 100
Gulbis, A. A. S., et al. 2006, Nature, 439, 48
Massey, P., & Jacoby, G. H. 1992, in ASP Conf. Ser. 23, Astronomical CCD Observing and Reduction Techniques, ed. S. B. Howell (San Francisco: ASP) 240
McDonald, S. W., & Elliot, J. L. 2000, AJ, 119, 1999
Person, M. J., et al. 2008, AJ, 136, 1510
Souza, S. P., Babcock, B. A., Pasachoff, J. M., Gulbis, A. A. S., Elliot, J. L., Person, M. J., & Gangestad, J. W. 2006, PASP, 118, 1550
Stansberry, J., Grundy, W., Brown, M., Cruikshank, D., Spencer, J., Trilling, D., & Margot, J. 2008, The Solar System Beyond Neptune, ed. M. A. Barucci, H. Boehnhardt, D. P. Cruikshank, & A. Morbidelli (Tucson: University of Arizona Press) 161